

City Research Online

City, University of London Institutional Repository

Citation: Nouri, J. M., Guerrato, D., Stosic, N. & Yan, Y. (2025). Suction Flow Measurements in a Twin-Screw Compressor. Fluids, 10(10), 265. doi: 10.3390/fluids10100265

This is the published version of the paper.

This version of the publication may differ from the final published version.

Permanent repository link: https://openaccess.city.ac.uk/id/eprint/36224/

Link to published version: https://doi.org/10.3390/fluids10100265

Copyright: City Research Online aims to make research outputs of City, University of London available to a wider audience. Copyright and Moral Rights remain with the author(s) and/or copyright holders. URLs from City Research Online may be freely distributed and linked to.

Reuse: Copies of full items can be used for personal research or study, educational, or not-for-profit purposes without prior permission or charge. Provided that the authors, title and full bibliographic details are credited, a hyperlink and/or URL is given for the original metadata page and the content is not changed in any way.

City Research Online: http://openaccess.city.ac.uk/ publications@city.ac.uk/





Article

Suction Flow Measurements in a Twin-Screw Compressor

Jamshid Malekmohammadi Nouri 1,*, Diego Guerrato 2, Nikola Stosic 1 and Youyou Yan 1

- School of Science & Technology, Department of Engineering, Mechanical Engineering and Aeronautics, City St George's, University of London, London EC1V OHB, UK; n.stosic@citystgeorge.ac.uk (N.S.)
- ² Delphi Diesel System, Courteney Rd., Gillingham ME8 0RU, UK; diego.guerrato@de.com
- * Correspondence: j.m.nouri@citystgeorge.ac.uk; Tel.: +44-(0)-7552501549

Abstract

Mean flow velocities and the corresponding turbulence fluctuation velocities were measured within the suction port of a standard twin-screw compressor using LDV and PIV optical techniques. Time-resolved velocity measurements were carried out over a time window of 1° at a rotor speed of 1000 rpm, a pressure ratio of 1, and an air temperature of 55 °C. Detailed LDV measurements revealed a very stable and slow inflow, with almost no influence from rotor movements except near the rotors, where a more complex flow formed in the suction port. The axial velocity near the rotors exhibited wavy profiles, while the horizontal velocity showed a rotational flow motion around the centre of the port. The turbulence results showed uniform distributions and were independent of the rotors' motion, even near the rotors. PIV measurements confirmed that there is no rotor movement influence on the inflow structure and revealed complex flow structures, with a crossflow dominated by a main flow stream and two counter-rotating vortices in the X-Y plane; in the Y-Z plane, the presence of a strong horizonal stream was observed away from the suction port, which turned downward vertically near the entrance of the port. The corresponding turbulence results in both planes showed uniform distributions independent of rotor motions that were similar in all directions.

Keywords: twin-screw compressor; suction flow; LDV and PIV optical techniques; angle-resolved averaging; mean and RMS velocities



Academic Editor: Jun Yao

Received: 9 August 2025 Revised: 1 October 2025 Accepted: 4 October 2025 Published: 11 October 2025

Citation: Nouri, J.M.; Guerrato, D.; Stosic, N.; Yan, Y. Suction Flow Measurements in a Twin-Screw Compressor. *Fluids* **2025**, *10*, 265. https://doi.org/10.3390/ fluids10100265

Copyright: © 2025 by the authors. Licensee MDPI, Basel, Switzerland. This article is an open access article distributed under the terms and conditions of the Creative Commons Attribution (CC BY) license (https://creativecommons.org/licenses/by/4.0/).

1. Introduction

The present investigation is concerned with the measurement of the mean axial and horizontal velocity components, their corresponding velocity fluctuations (RMS), and velocity vectors in the axial and horizontal planes within the suction port of a twin-screw compressor using laser Doppler velocimetry (LDV) and particle image velocimetry (PIV) techniques. This study is a continuation of earlier work by the current authors [1], where the application of LDV and PIV techniques was investigated for accurately measuring flow behaviours in a screw compressor, and a small sample of data was presented with respect to a suction port. Screw compressors are used widely in different industrial applications, like air compression, refrigerant compression, food processing, pneumatic transport, automotive uses, turbocharging, and pharmaceutical processes [2–11], mainly due to their simple design, low manufacturing cost, long service life, low vibration, and high transmission efficiency. These machines can operate over a wide range of speeds and pressures. Yet, machine developers, manufacturers, and researchers are continually challenged to broaden the scope of their applications and improve both design and efficiency, especially for compressors that are capable of handling single-phase and multi-phase fluids [3,12]. The screw

machine used in this study is an 'N'-type rotor profile with a 5/6 lobe configuration and consists of two rotors (male and female) contained in a casing with no valves; their meshing lobes form a number of working chamber flows (five here), within which compression takes place, as described in [3]. The compression process continues as the chamber flows (five times within a full cycle) move from the suction port towards the exit, where high-pressure flow is exposed to the discharge port and is then released into the discharge cavity [3–5].

The design optimisations and basic operations of screw compressors have been studied by many researchers [4,5] via analytical methods and experimental testing, and they are well established. Recent works [6–11] on screw compressors include progress in component manufacturing [6], including cutting processes, solid plastic forming, casting, and additive manufacturing, which can enable the fabrication of screw rotors via a closed extrusion process. A recent review of numerical simulation research on the internal flow and performance optimisation of screw compressors was conducted by the authors of [7], where different flow modelling methods regarding structural operating conditions and performance optimisation were discussed, and the synergistic potential between these technologies was investigated. One study [8] presented a CFD analysis using SolidWorks for the optimisation of parameters such as rotor profiles, rotor speeds, clearance gaps, and thermal effects, which can be easily adopted in different types of screw compressors. Rotor thermal deformation was studied by the authors of [9], who used different methods to show the significant impact of thermal deformation on the clearances between the working elements of the compressor during the design process. The optimisation of rotor profiles in screw compressors was recently [10] investigated using a machine learning (ML) optimizer to explore the design space of screw profiles, coupling geometric manipulation with compressor performance estimation. Finally, the use of water as a refrigerant for chiller and heat pump applications with screw compressors was studied in [11] due to its environmental friendliness and wide availability. They varied the design and materials of the rotor assembly to explore the influence of these modifications on structural performance and identified excitation sources, and used the Campblee diagram to visualise potential resonances and the critical speed of the presented assemblies.

However, the information on the flow processes within compressors at all stages, from suction to discharge, is fairly limited. A full understanding of the flow processes (obtained by measurements or CFD simulations) within compressors would greatly help to improve the design and performance of screw machines [5]. In fact, this information can be used as an integrated part of the design and optimisation processes [7,13,14], and as shown by recent flow simulation results [7], the role and potential of deep exploration into the intrinsic relationship between local complex flow characteristics and structural optimisation for performance improvement of twin-screw compressors is essential. Thus, the current research project was designed to measure flow characteristics throughout the compressor, from suction to discharge, using optical diagnostics like high-speed flow visualisation, LDV, and PIV techniques. Flow measurements at different parts of the compressor (within the rotors' working chambers [12,15], near the inlet and outlet of the discharge port [16], and within the discharge cavity up to the exhaust [17]) have been reported by the current authors, and the results presented in this report is the last stage of this research project. The current results are original, and to the authors' knowledge, there are no such detailed flow measurements (in the literature) in twin-screw compressors using LDV and PIV methods. The use of optical diagnoses (flow visualisation, LDV, and PIV techniques) is essential for flow characterisation in complex geometries like compressors and IC engines, as explained in detail in previous reports [15–18]. Optical probes provide proper access into the flow domains without compromising the integrity of the flow configurations, and they allow for

accurate data measurement of real-time flow dynamics. This has also been supported by critical reviews of experimental studies related to twin-screw compressors [19] and other complex geometries, which have recommended the use of optical visualisation techniques such as LDV/PIV for flow field characterisation. More importantly, these results can be used to validate CFD simulations, which is the best approach for fully characterising the real-time fluid flow, offering substantial reductions in time and cost compared with an experimental-based approach [2,7].

The flow process within the rotors' working chambers depends significantly on the inflow structure from the suction port, the shape of the suction port, and the flow trajectory as it enters the rotor chambers [13]. Equally, the compressor performance is highly affected by flow behaviour within the suction port, rotor chamber, and discharge port; in particular, flow losses in the suction port can lead to a decrease in compressor efficiency as shown by [14,20], who also discussed the impact of the flow leakages between the rotors and casing, which are dependent on various clearances and pressure differences across them. However, the new profiling techniques ensure the manufacture of rotors profiles, even the most complex shapes, to tolerances on the order of a few microns, thereby achieving high efficiencies [3,13]. Recent CFD and PIV studies [21,22] investigated the tip leakage gap between the rotor and housing of a Roots Blower (rotary positive displacement machine) for different rotor tip designs and clearances. PIV results showed that the leakage flows were sensitive to rotor speed and that the predicted discharge flow and temperature deviations from the experiment were within 7%. A numerical study [23] on a screw compressor investigated the leakage flow, pressure, and temperature distributions on both male and female rotors during compression and expansion processes, and it revealed that the volumetric efficiency slightly decreased when the wrap angle increased during the compression process. Overall, flow processes in compressors are complex, 3D, highly turbulent, and periodic. It is, therefore, essential to have a good understanding of the flow motion characteristics within the compressors, as acknowledged in a recent review by [7]. This can be realised through accurate experimental flow measurements and validated CFD simulations throughout the compressor, from suction to discharge sections.

Although limited, a number of previous investigations have been carried out (as mentioned above) to examine the flow behaviour within rotor chambers, the discharge cavity, and leakage flow using different experimental methods and CFD simulations. The flow within the suction port and its upstream region remains fairly unexplored, except for a few publications that show that CFD can be effectively used to analyse the flow in the suction port of a screw compressor, as reported by [2], who also visualised the flow using a high-speed camera and compared it with CFD predictions. Similar approaches were used by [13,14] to predict flow losses [14], and they showed the possibility of improving efficiency through a simple change in the design of the suction plenum [13], although they concluded that the introduction of a radial suction port showed no improvement in compressor performance compared to the standard axial port. Therefore, the main objective of current study is to use LDV and PIV methods to measure the mean and RMS velocities upstream of and near the suction port. The design of the compressor, its setup, optical arrangements, and data processing are fully described in [1].

Thus, the present report is an experimental research work on flow characterisation within a standard axial suction port, which contains an original set of data that is being published for the first time and presents a new contribution to the literature. The flow through the modified optical suction port has been measured as close as possible to the rotors using LDV and PIV techniques. Time-resolved (cycle-resolved) mean and RMS velocity variations have been obtained within the suction port to characterise the flow sequences, especially when the flow moves from the port into the male and female rotors.

Fluids **2025**, 10, 265 4 of 21

The newly measured data have been obtained in great detail to support the validation of CFD codes, aiming to establish a reliable model for accurate prediction of flow and pressure distribution within twin-screw machines; this model can be used as a tool to further improve the design of screw compressors and expanders. The current measurements were performed at the inlet of the suction port by passing the laser beams (LDV) and a laser sheet (PIV) through especially designed transparent windows made of Plexiglas (Perspex), which were installed on top of the suction port casing; full details are given in [1], and a brief summary is provided in the following section. The results are presented and discussed in the subsequent section, and the report concludes with a summary of the main findings.

2. Flow Configuration and Instrumentation

Figure 1 shows LDV and PIV setups at the suction port of a twin-screw compressor. The compressor had 'N'-type rotor profiles and was operated at a rotor speed of 1000 rpm, a pressure ratio of 1, and a gas temperature of 55 °C. To make the suction port optically accessible, the suction pipe was replaced by a transparent cylinder fitted on top of the machine's inlet port; the cylinder had a height of 170 mm and an inner diameter of 106 mm (the same as suction diameter), as shown in Figures 1 and 2. The other end of the cylinder was covered by a flat transparent window (above the feeding pipe, which had an inner diameter of 60 mm), which provided sufficient optical access into the suction port for both LDV and PIV measurements; see Figure 3 for PIV optical arrangements. Figure 2 shows the modified optical suction port along with the adopted coordinate system. The Z axis was aligned with the axis of the vertical cylinder with its zero located at the entrance of the compressor inlet port above the rotor chamber. The X axis was aligned with the rotor shaft, with its positive (+ve) direction pointing towards the main shaft, and the Y axis was perpendicular to both the X and Z planes, with its +ve direction pointing from the female to the male rotor. The dark grey spots in Figure 2 correspond to LDV measurement points at three vertical locations: Z = -10, 5, and 75 mm. Z = -10 mm is the closest plane to the rotors, Z = +5 mm is the entrance of the suction port, and Z = +75 mm is the upstream location of the suction pipe. X- and Y-components of velocity (referred to as axial velocity, Vx, and horizontal velocity, Vy, respectively) were easily measured from the top flat window, while the vertical velocity (Z-component, Vz) was measured through the diagonal planes of the vertical cylinder. The Vz measurements were only possible at Z = 75 mm; measurements at Z = 5 and Z = -10 mm were not possible because the laser beams could not access those locations due to the presence of the metallic compressor walls. This limitation can be addressed by modifying the inlet casing and inserting small optical windows on the diagonal plane. Alternatively, one can cut the entire inlet flange of the suction port down to just above the splitter bridge (see Figure 4a) of the rotors and replace it with an optical unit that allows access to the top of the rotors in the suction port; although difficult, this modification can be feasible.

LDV and PIV systems used were the same as those described by [5,24] and will not be repeated here. A conventional silicon oil atomizer with an average droplet size of 1–2 μm was used as the flow tracer. This is the most common air flow tracer used for LDV techniques and has also been shown to be suitable for PIV measurements in [24], enabling good data processing using the cross-correlation method. Seeding was introduced into the suction port from the inlet feeding pipe, as shown in Figure 2. One of the disadvantages of using the silicon oil droplets is the fouling of optical windows, especially during rotor and discharge flow measurements, where the windows have to be cleaned every 20 min [5]. However, in the suction port, this was not found to be a major issue mainly due to the more uniform and stable flow nature of the suction port. In this study, the experiment could run for over an hour (70–80 min) without any signal deterioration; to be on the safe side, the

Fluids **2025**, 10, 265 5 of 21

windows were cleaned regularly every 45–50 min. It has been shown in [25,26] that better results can be obtained by using CO_2 solid particles as seeding, introduced through the suction port.

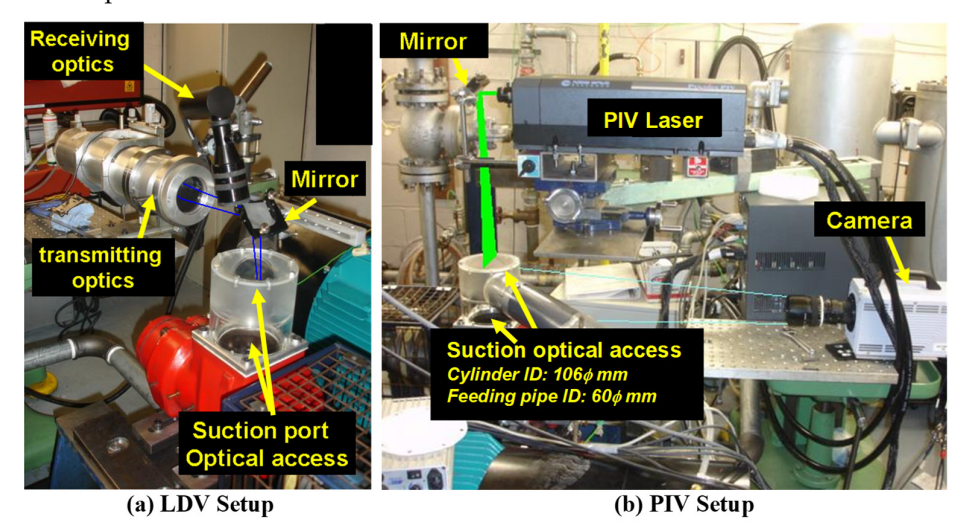


Figure 1. Modified compressor at the suction port with transparent inlet pipe for LDV and PIV measurements.

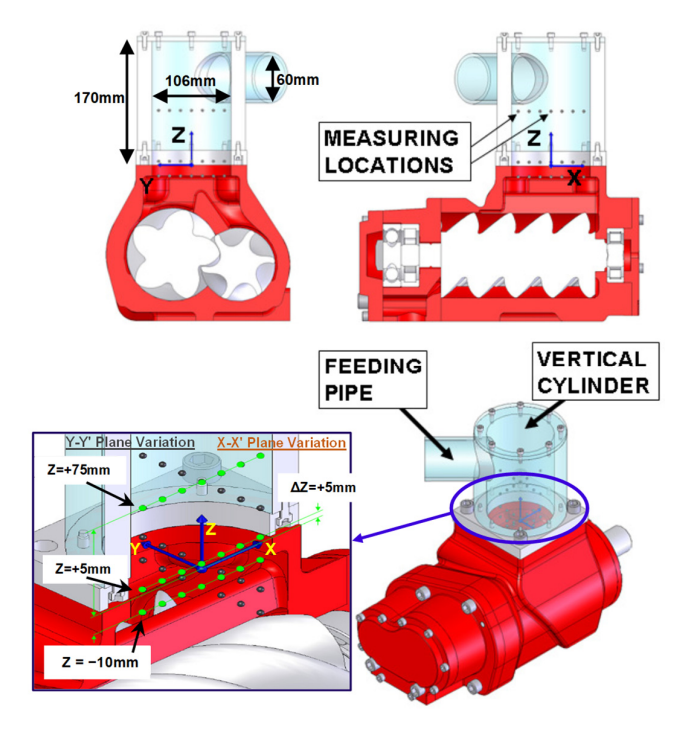


Figure 2. Screw compressor and suction port views with the adopted coordinate system.

LDV measurements include angle-resolved mean and RMS velocity variations of the vertical (Vz), axial (Vx), and horizontal (Vy) components along the diagonal X (X-X') and Y axes (Y-Y'), as shown in Figure 2, at different Z locations. Although LDV measurements provide highly accurate information about mean and turbulence velocities, particularly the latter, it is a point-based measuring system; hence, obtaining detailed flow characteristics across every fluid domain is very time-consuming. Thus, PIV is an alternative measuring technique that can capture instantaneous flow field velocity (2D or 3D) within a plane and provide useful information regarding spatial gradient and Reynolds stresses throughout the measuring plane. Therefore, a 2D PIV system was used to map the flow within the inlet suction port in both horizontal and vertical planes, as shown schematically in Figure 3. The

transmitting PIV laser sheet was passed horizontally (Figure 3a) or vertically (Figure 3b) through the optical cylinder and top window, either directly or through a 45° mirror. With this arrangement, all three velocity components could be measured, but this required different PIV setups. The receiving PIV optics were aligned to collect the data through the flat window and vertical cylinder for the horizontal (Figure 3a) and vertical (Figure 3b) plane measurements, respectively.

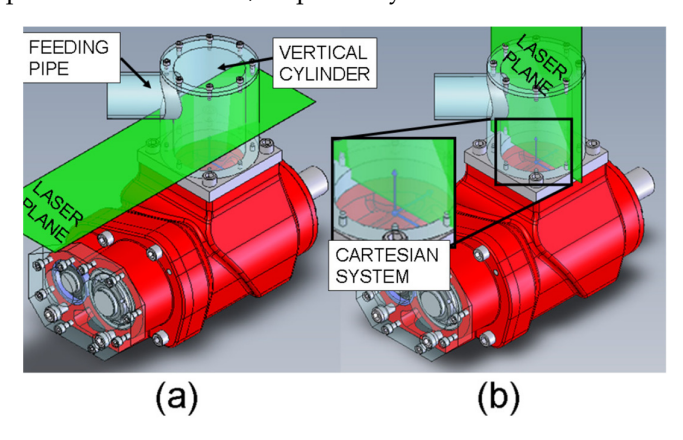


Figure 3. Schematic presentation of the PIV optical arrangements: (**a**) horizontal plane for measuring instantaneous vector velocity in the X-Y plane; (**b**) vertical plane for measuring instantaneous vector velocity in the X-Z and Y-Z planes.

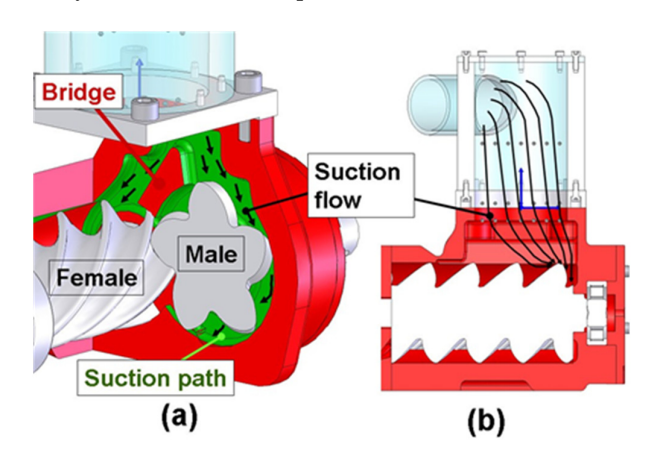


Figure 4. Schematic description of suction flow within (a) the compressor inlet and (b) the suction port.

Although the errors and uncertainties in measured data were explained fully by [5,24], who used the same optical systems, a brief summary is provided here. For LDV measurements, 2000 to 3000 samples were collected at each point over 1° time window (data were collected continuously over many shaft cycles until the required number of samples were achieved) to ensure high level of convergence for both mean and RMS velocities with a maximum statistical error of 0.8% in the ensembled mean and 2.5% in the RMS of velocity fluctuations for a 20% turbulence intensity; the accuracy would be even higher for flows at a lower turbulence intensity, like the suction flow investigated here. For PIV measurements, 30 images were used to compute the mean velocity vector field. To examine the accuracy of the measured PIV data, a comparison between LDV and PIV measurements was carried out by the current authors [17] at the exit of the discharge port of the compressor, where the flow is highly turbulent, 3D, periodic, and characterised by large mean velocity variations and very steep velocity gradients. The results showed very good agreement in mean velocities between the two methods at most angular locations. However, discrepancies existed with maximum differences of up to 20% at some angular

Fluids 2025, 10, 265 7 of 21

locations, particularly after the opening of the discharge port ($0^{\circ} < \theta > 20^{\circ}$), where the temporal and spatial mean flow gradients were the largest. These differences can be due to statistical uncertainties, as averaging over a 1° time window is carried out using 30 samples, compared to those of LDV, which use at least a few thousand samples. This provides a good level of confidence in the accuracy of the measured PIV mean velocity results, and especially for measurements in the suction port, where the flow is less turbulent and more stable.

On the other hand, in the turbulent flow, there are uncertainties associated with PIV measurements, in accurately capturing the turbulence structure, mainly due to the larger pulse separation time (Δt) compared to other optical flow velocimetry like LDV, and also due to high statistical error caused by the small number of samples measured per location, which is restricted (30 images in this experiment) [5,27]. It was argued by [27] that with PIV measurements, care should be taken when drawing conclusions from vectors with small magnitudes because the smallest resolvable displacement does not remain constant as the largest displacements increase with increasing Δt . Overall, the turbulence results obtained in this experiment do not represent the true turbulent behaviour quantitatively due to the aforementioned systematic errors, and for that reason, LDV turbulence results are more reliable than PIV ones. However, some samples of PIV turbulence velocity fluctuation results are presented here to show the variation of RMS velocities qualitatively, in order to have a better understanding of the turbulence structure and also to see whether they follow similar pattern to that of LDV results.

3. Results and Discussion

The suction flow geometry is complex, which makes it difficult to understand the measured flow behaviour; thus, a description of the inlet flow geometry is essential. A schematic description of the suction port, from optical cylinder to the rotors, is shown in Figure 4. The suction port geometry in Figure 4a shows a bridge above the rotors that splits the incoming flow towards the male and female rotors, following the flow passages between the bridge and the casing. With the present optical arrangement, unfortunately, it was not possible to measure the flow around the bridge to show the effect of rotor rotation on the suction flow, and the closest location where measurements were optically possible was at Z = -10 mm, where the following results show the effect of rotor motion on the flow. However, the suction flow in the optical cylinder (as depicted in Figure 4b) is expected to be mainly vertically downward towards the suction port. Since there are five opening/closing operations of the discharge port during a full rotational cycle, the flow velocity measurements over one opening/closing cycle are presented (i.e., 72° of the main shaft rotation), with the assumption that the flow over the other four are repetitive and similar. It should be noted that the opening of the discharge port corresponds to a main shaft angle of $\theta = 0^{\circ}$ [16], where the high-pressure flow begins to enter the discharge port, causing a sudden and rapid change in flow velocity. In order to locate this position and synchronise the velocity measurements with respect to the location of the rotor, a shaft encoder was used, which provides 1 pulse per revolution and 3600 train pulses; this is the same for all LDV and PIV measurements. In the following sections, LDV results are presented first, followed by PIV results, and they show the behaviour of the mean velocities and their corresponding turbulence fluctuations as a function of the shaft angular position, θ , within the suction port.

3.1. LDV Results

The velocity profiles presented in Figures 5–9 are cycle-averaged over a one-degree time window ($\Delta\theta = 1^{\circ}$), and are obtained from continuous measurements with respect to

shaft rotation over many 360° , until sufficient samples are collected to provide accurate (statically) mean and RMS velocities over each one-degree time window. The mean vertical flow velocity (Vz) at Z=+75 mm are presented and discussed first to illustrate the main downward flow within the optical cylinder, which can be considered the main inlet flow to the suction port. Then, the mean and RMS velocity variations of axial (Vx) and horizontal (Vy) velocity components at Z=-10 mm +5 mm are presented, which are the main focus of the current study, as Z=+5 mm represents the upstream flow entering the suction port, and Z=-10 mm represents the flow within the suction port close to the rotors. As mentioned before, measurements of the main vertical flow velocity, Vz, was not possible at Z=-10 mm +5 mm due to obstruction of the laser beams by the suction port wall.

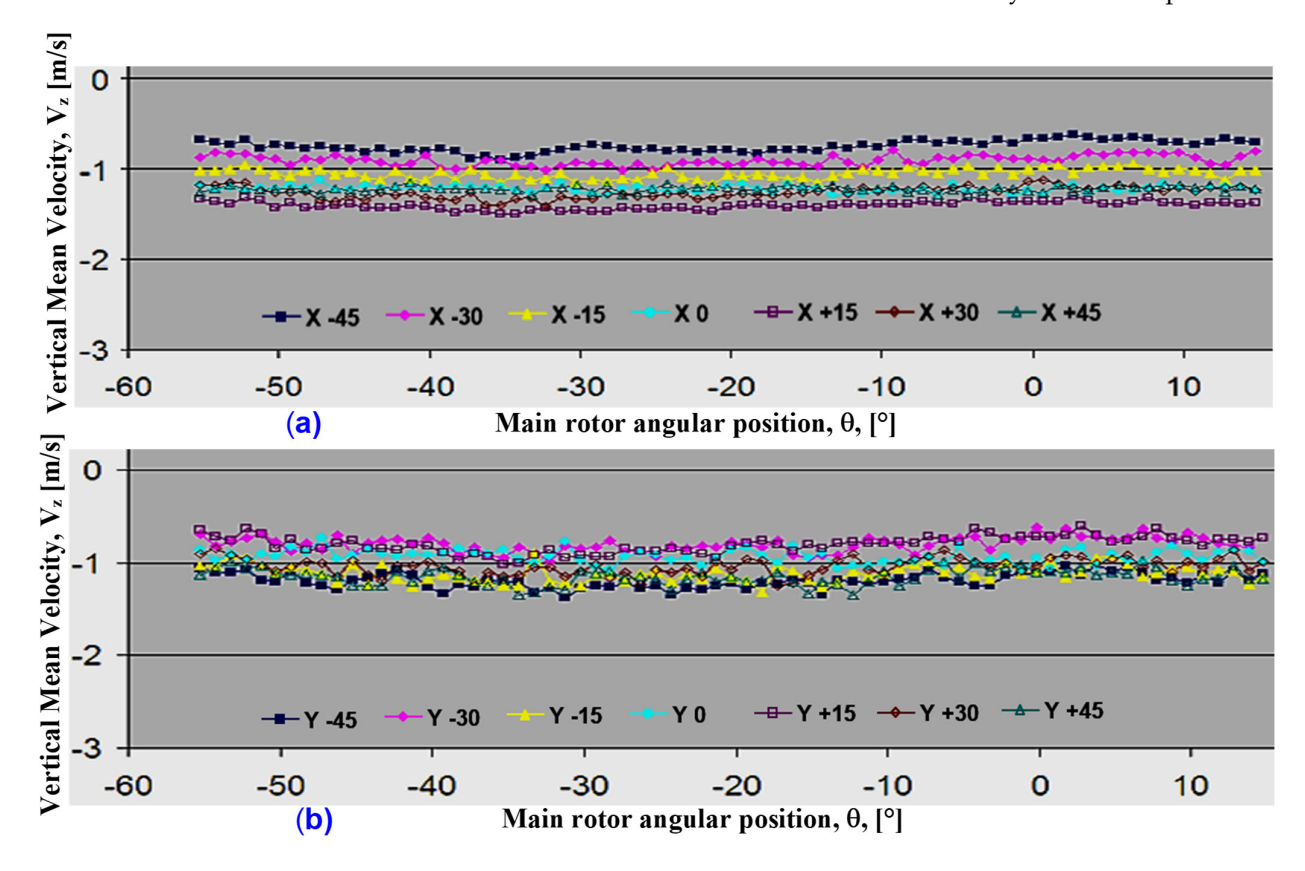


Figure 5. Variation of vertical (Vz) mean velocity as a function of rotor angle, θ , at Z = +75 mm for (a) different X-locations along the X-X' axis at Y = 0 mm and (b) different Y-locations along the Y-Y' axis at X = 0 mm.

Figure 5 presents the variation of the mean vertical velocity, Vz, as a function of θ , at Z = +75 mm along the X-X' (different X-locations, Figure 5a) and Y-Y' axes (different Y-locations, Figure 5b). The results show uniform downflow (negative Vz values towards the rotors) velocity profiles along both the X-X' and Y-Y' axes at different X- and Y-locations, respectively, with no observable influence from the rotors' rotational motion, as would be expected at z = +75 mm. The downflow vertical velocity along the X-X' axis, shown in Figure 5a, varies at different X-locations such that it is around -0.7 m/s at X = -45 mm (near cylinder wall), then increases gradually with X to a maximum value of around -1.4 m/s at X = +15 mm, and then drops to -1.2 m/s at X = +45 mm (near the opposite cylinder wall); this variation along X-X' axis suggests that the incoming flow from the feeding pipe into the cylinder has not developed fully at this Z location. Figure 5b shows similar downflow along the Y-Y' axis at different Y-locations with smaller variation in Vz values compared to that observed along the X-X' axis, and no obvious trend, with an overall average value of around -1 m/s. The corresponding RMS velocity fluctuations,

not presented here, showed similarly uniform profiles along both the X-X' and Y-Y' axes, with an average value of around 1 m/s.

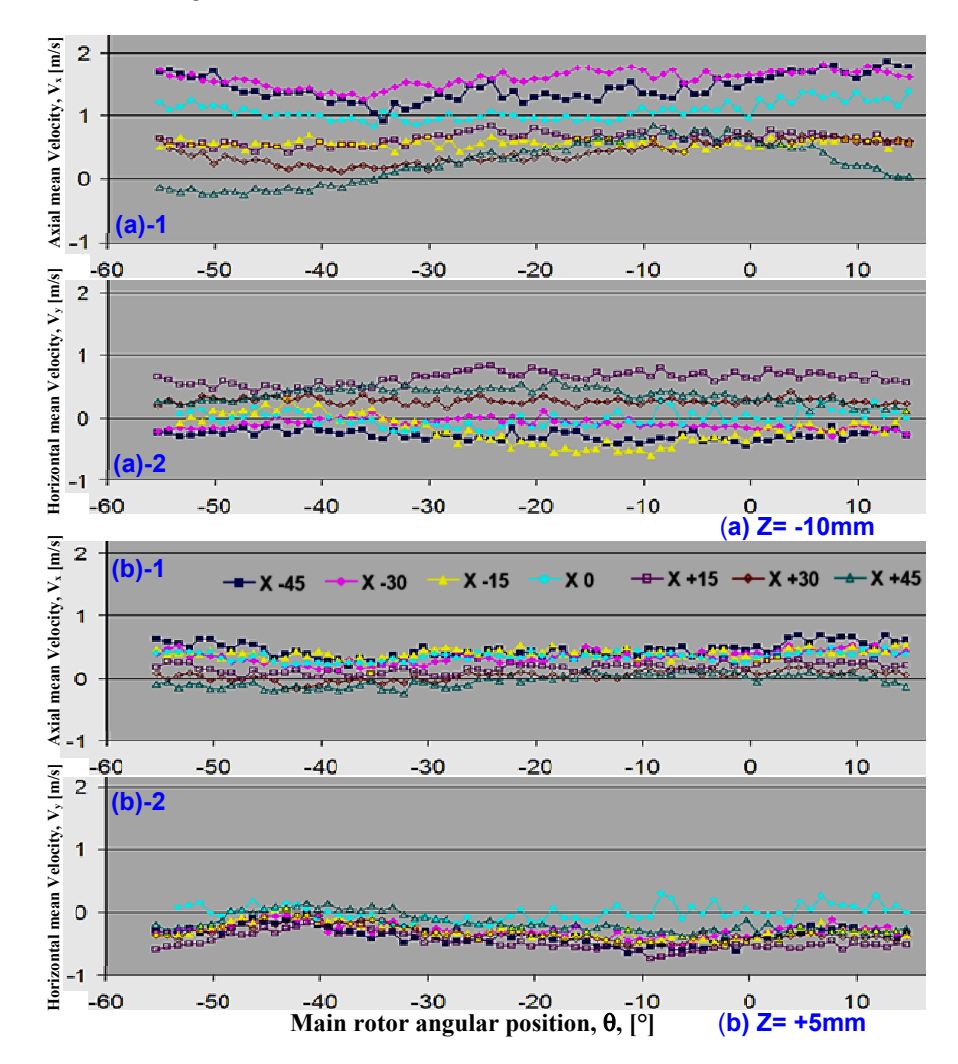


Figure 6. Variation of axial (Vx) and horizontal (Vy) mean velocities as a function of rotor angle, θ , for different X-locations along the X-X' axis at Y = 0 mm, and at (a) Z = -10 mm and (b) Z = +5 mm.

The mean axial, Vx, and horizontal, Vy, velocity profiles as a function of θ along the X-X' axis are shown Figure 6 at Z=-10 mm (Figure 6a) and Z=+5 mm (Figure 6b). Note that the graphs in Figure 6((a)-1,(b)-1) represent the axial velocity profiles, while the graphs in Figure 6((a)-2,(b)-2) represent the horizontal velocity profiles; the same arrangements are used in Figures 7–9. Starting from the vertical location of Z=+5 mm, Figure 6b, just above the suction port entrance, the results show uniform axial and horizontal velocity profiles with θ , suggesting little or no influence of the rotors' rotational motion at this vertical location. Also, the profiles at different X-locations appear similar, with the axial velocity tending to be positive, up to 0.7 m/s, especially at negative X-locations (where the flow is more exposed to rotors chambers), while the horizontal velocity tends to be negative, up to -0.7 m/s, suggesting a slow flow motion from the male rotor side to the female rotor along the X-X' axis at this vertical location.

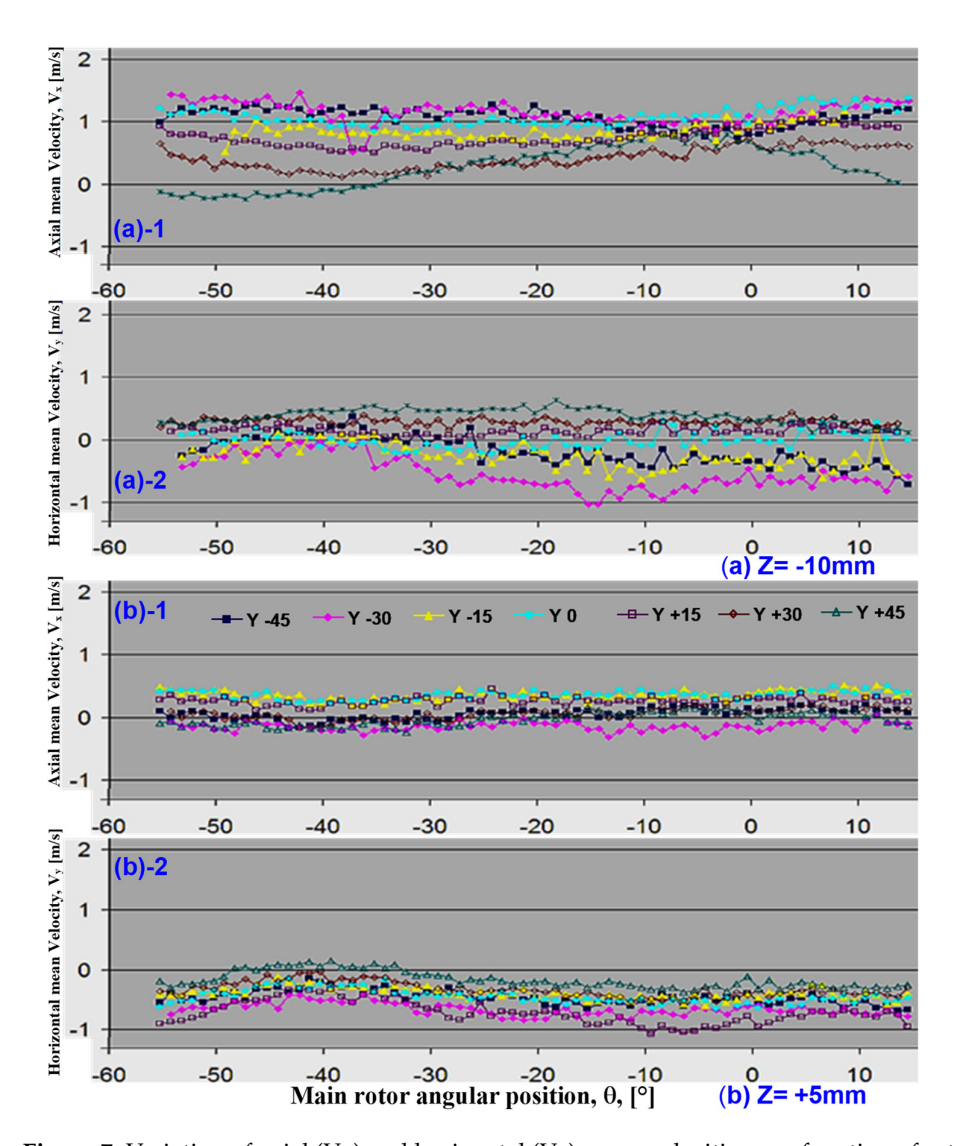


Figure 7. Variation of axial (Vx) and horizontal (Vy) mean velocities as a function of rotor angle, θ , for different Y-locations along the Y-Y' axis at X = 0 mm, and at (a) Z = -10 mm and (b) Z = +5 mm.

Further downstream at Z = -10 mm within the suction port and closer to the rotors, Figure 6a, both axial and horizontal velocities are influenced by the X-locations of the control volume as well as by the shaft angle, θ . The latter is expected due to the close proximity of the measurement points to the rotors, where their motion interacts with the fluid flow and creates differences in pressure between the open working chambers and the suction port of the rotor. The axial velocity, Vx, is mainly positive, with the highest values, up to 1.8 m/s at X = -30 and -40 mm; the profiles look like a wave, which may indicate that the flow is moving towards a working chamber that is opening and absorbing fluid, but since more than one working chamber is connected to the suction port for each shaft angular position, interpretation of the flow behaviour becomes more difficult. Unlike the axial velocity, the horizontal velocity, Vy, shows a variation with X-locations: it shows positive values (towards the male rotor) and negative values (towards the female rotor) at positive and negative X-locations, respectively, with almost zero velocity at the centre, i.e., X = 0. This is more pronounced between shaft angles $\theta = -30^{\circ}$ to 10° , with Vy values reaching up to +0.8 m/s and -0.6 m/s. The fact that the velocity changes from negative to positive values suggests that there is a rotational flow movement with its centre close to the Z axis.

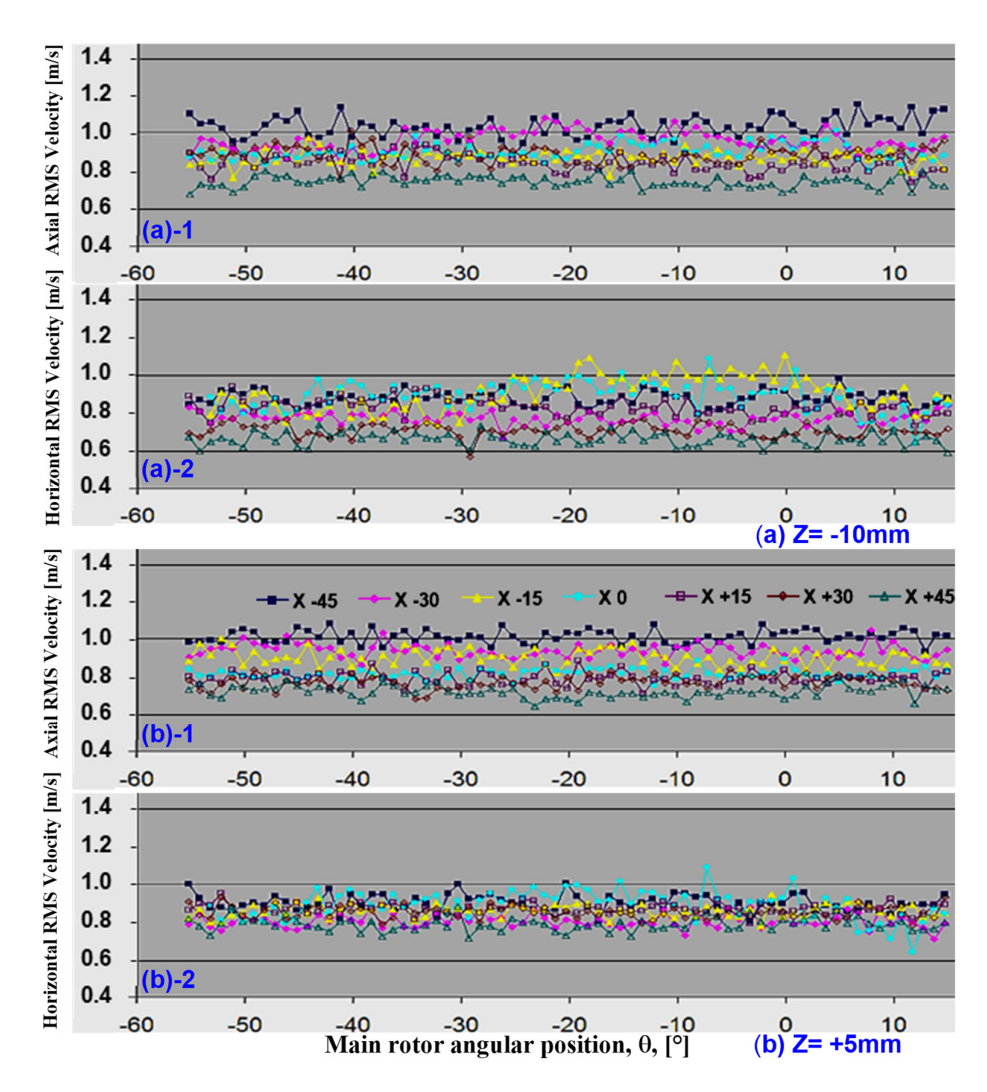


Figure 8. Variation of axial and horizontal turbulent velocities as a function of rotor angle, θ , for different X-locations along the X-X' axis at Y = 0 mm, and at (a) Z = -10 mm and (b) Z = +5 mm.

The variations of the mean axial, Vx, and horizontal, Vy, velocities with shaft angle, θ , along the Y-Y' axis at Z = -10 mm and +5 mm are shown in Figure 7. Similar results to those in Figure 6 can be seen here at Z = +5 mm, Figure 7b, with almost uniform axial and horizontal velocity profiles. The results show almost no influence from rotor motion, and the horizontal velocities are negative (Figure 7((b)-2)) with values up to -1 m/s, indicating flow from the male rotor towards the female rotor at all Y-locations. Closer to rotors at Z = -10 mm in Figure 7b, although similar trends to those in Figure 6b are observed in both Vx and Vy profiles, there are some differences. For example, the axial velocity, Vx, profiles at negative Y-locations (over the female rotor) become more uniform and reduce in value to around 1 m/s, while the velocity profiles at positive Y-locations (over the male rotor) are highly dependent on rotor angle, suggesting that the flow interaction by the male rotor is more dominant than that of the female rotor. Also, for the horizontal flow velocity, Vy, (Figure 7((a)-2)) similar positive and negative values (to those observed in Figure 6((a)-2)can be seen at positive Y- and negative Y-locations, respectively, but the velocity variations with θ at positive Y-locations became more uniform and reduced in magnitude, confirming the above observation that the female rotor movement in less dominant than that of the male rotor in influencing the flow within the suction port. As a consequence, it can be suggested that the male rotor interacts better with the inflow air within the suction port and therefore more air is flowing towards the male rotor. Overall, the results near the

rotors show the presence of a complex flow in the suction that includes an axial component moving down towards the working chambers at the front of the compressor (negative X), with the flow (on the left side of compressor (negative Y)) tending towards the centre of the female rotor, while more flow (on the right side (positive Y)) is directed to the male rotor, similar to the simplified flow description presented in Figure 4. This is due to the geometry of the suction port, which has been designed in such a way that causes the suction process to take place in this way.

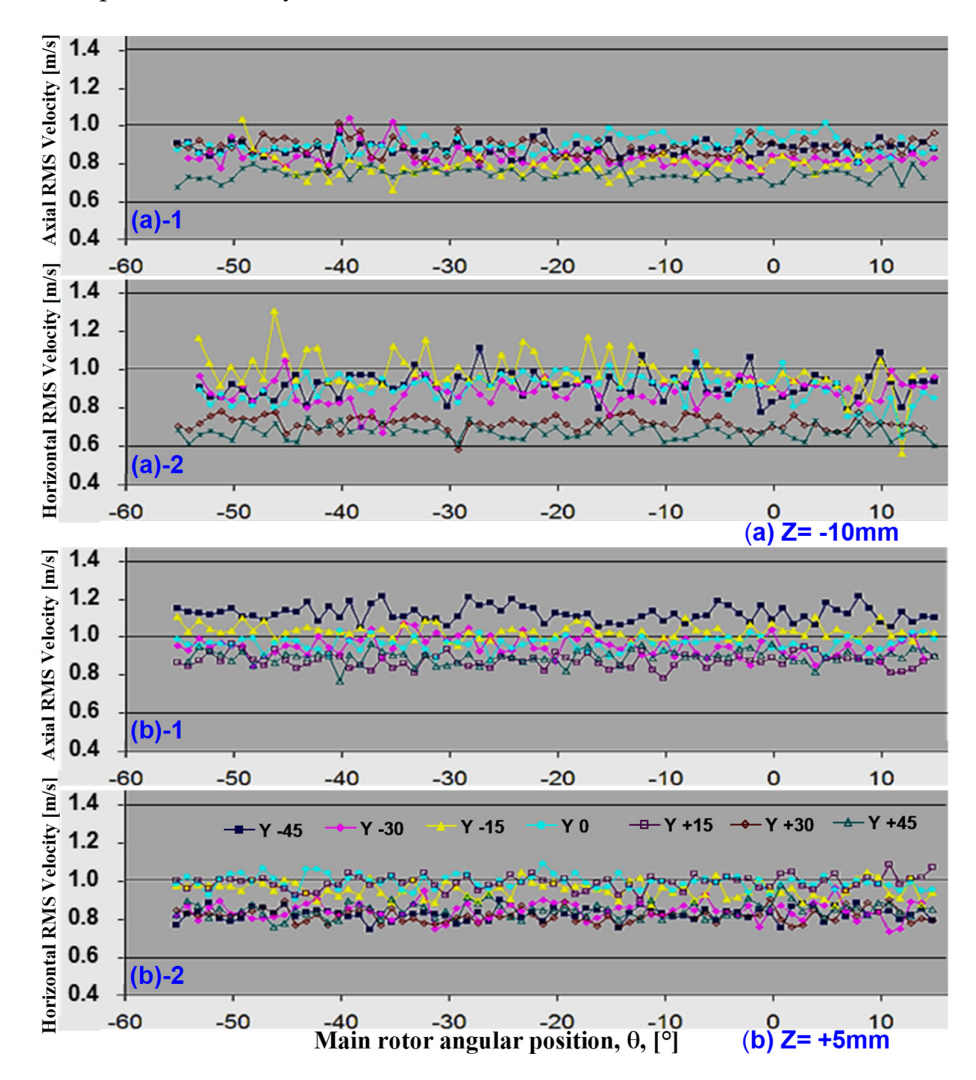


Figure 9. Variation of axial and horizontal turbulent velocities as a function of rotor angle, θ , for different Y-locations along the Y-Y' axis at X = 0 mm, and at (a) Z = -10 mm and (b) Z = +5 mm.

Figures 8 and 9 present the corresponding axial and horizontal RMS velocity fluctuation profiles, related to Figures 6 and 7, along the X-X' and Y-Y' axes, respectively. In general, the results show that the turbulence of both velocity components are uniform and independent of the shaft angle. This is particularly true at Z = +5 mm in Figures 8b and 9b, where the overall average turbulence level is around 1 m/s, with the axial RMS velocities being slightly higher than those of horizontal RMS values. Similar results can be seen even at Z = -10 mm, which is the closest position to the rotors (Figures 8a and 9a), except the fluctuations of horizontal RMS velocity (Figure 8((a)-2)and Figure 9((a)-2)), which are not due to the shaft rotation but rather due to the rotational mean flow velocity variations of positive and negative values, as explained in Figures 6 and 7. Overall, considering the similarity of both components obtained at Z = -10 mm, the results show that turbulence can be assumed to be almost isotropic. It is clear that the results provided here do not

include the vertical mean and RMS velocity components at Z = -10 mm, which would provide a clearer picture of the full inlet flow. Thus, it is recommended to modify the optical suction port to allow greater optical access to the suction port to include both mean and RMS values for the vertical velocity, Vz, at Z = -10 mm or even closer to the rotors. Furthermore, since the vertical velocity component is perpendicular to the suction port, it is important to have this information as it is responsible for feeding air flow into the compressor.

3.2. PIV Results

Although the LDV measurements presented in Figures 5-9 provide valuable insight into the mean and turbulent flow behaviour within the suction port, more measurement are required to fully describe the flow structure, which would be very time-consuming, as explained before. Nevertheless, the LDV results not only provide highly accurate information about the mean and turbulence velocities variations within suction port, but also provide ideal data to be used as input data for CFD simulations, and more importantly, to validate the CFD results for mean and turbulent flow with a high level of accuracy. To overcome the limitations of LDV measurements, a 2D PIV system was used (as described in the previous section in Figures 1-3) to capture instantaneous flow field velocity in a plane and provide useful spatial data of mean flow (vector velocities) and turbulent flow (contours of RMS velocities) everywhere within the measurement plane. It is worth mentioning that, since the suction port can be designed to be more optically accessible than the rest of the compressor (as mentioned before), and since the flow is more stable and less turbulent (as confirmed by above LDV measurements, and therefore less window fouling), the measurement period can be extended to obtain enough samples for better confidence in the accuracy of the PIV measurements.

The PIV measurements presented here were recorded for different planes with respect to the shaft angle, θ . Then, the velocity results were averaged to acquire the mean vector velocity and the corresponding turbulent velocity fluctuations over a time window of 1° $(\Delta\theta)$, using a customised special software; in this process, 30 images were used to compute the mean velocity vector field, with an average standard deviation of 10% of the mean value, in agreement with the LDV results. Figure 3 presents the two measuring configurations used herewith: Figure 3a presents the arrangement for measuring the flow at the green laser sheet in the X-Y plane (cross flow) localized at Z = 75 mm, the same plane used for LDV measurements; this position was particularly chosen to be far from the rotors. Figure 3b shows the vertical laser sheet along with the Y-Z plane, which is perpendicular to the rotors and represents downward flow into the rotors. The results from eight selected PIV images at different main shaft angles, θ , are chosen (before and after discharge opening) to describe the flow behaviour, and the results are shown in Figures 10 and 11. Note that the vector flow images might not be as clear as those obtained for the discharge flow [17], mainly due to the small magnitude of the velocities in the suction port, which are an order of magnitude smaller than those found in the discharge chamber, and secondly, the flow is more stable and almost independent of rotor angle.

Figure 10 presents the distribution of mean crossflow vector velocity $\left(\sqrt{V_x^2+V_y^2}\right)$ of the axial and horizontal velocity components within the X-Y plane for eight different shaft angles, θ , at Z=75 mm. Ideally, when the inlet pipe flow is fully developed, the velocity vectors are expected to be vertically downwards and uniform, with no or little crossflow. However, the crossflow results presented in Figure 10 at Z=+75 mm show a more complex, vortical, and three-dimensional flow; this was also observed from the LDV vertical (Vz) velocity results in Figure 5 at Z=+75 mm, which showed variation in velocity distributions along both the X and Y axes. This is mainly due to underdeveloped feeding flow in the

cylinder; here, the air enters through a horizontal feeding pipe into the transparent vertical cylinder, where it turns and moves down into the vertical cylinder towards the rotors. This change in feed flow direction requires more space and time to become fully developed and is the main cause of this unexpected result. A similar crossflow flow structure can be seen at all shaft angles, θ , (before and after the opening of the discharge port, i.e., $+\theta$ and $-\theta$), confirming that there is no influence of the shaft movement on the flow structure. The flow features in all graphs exhibit a main crossflow stream moving diagonally towards the top right corner with vector velocities up to 2 m/s, and the presence of two counter-rotating vortices at the top left and bottom right of all images. The results also show the presence of a third vortex formed in the bottom left, although it is weaker than the other two.

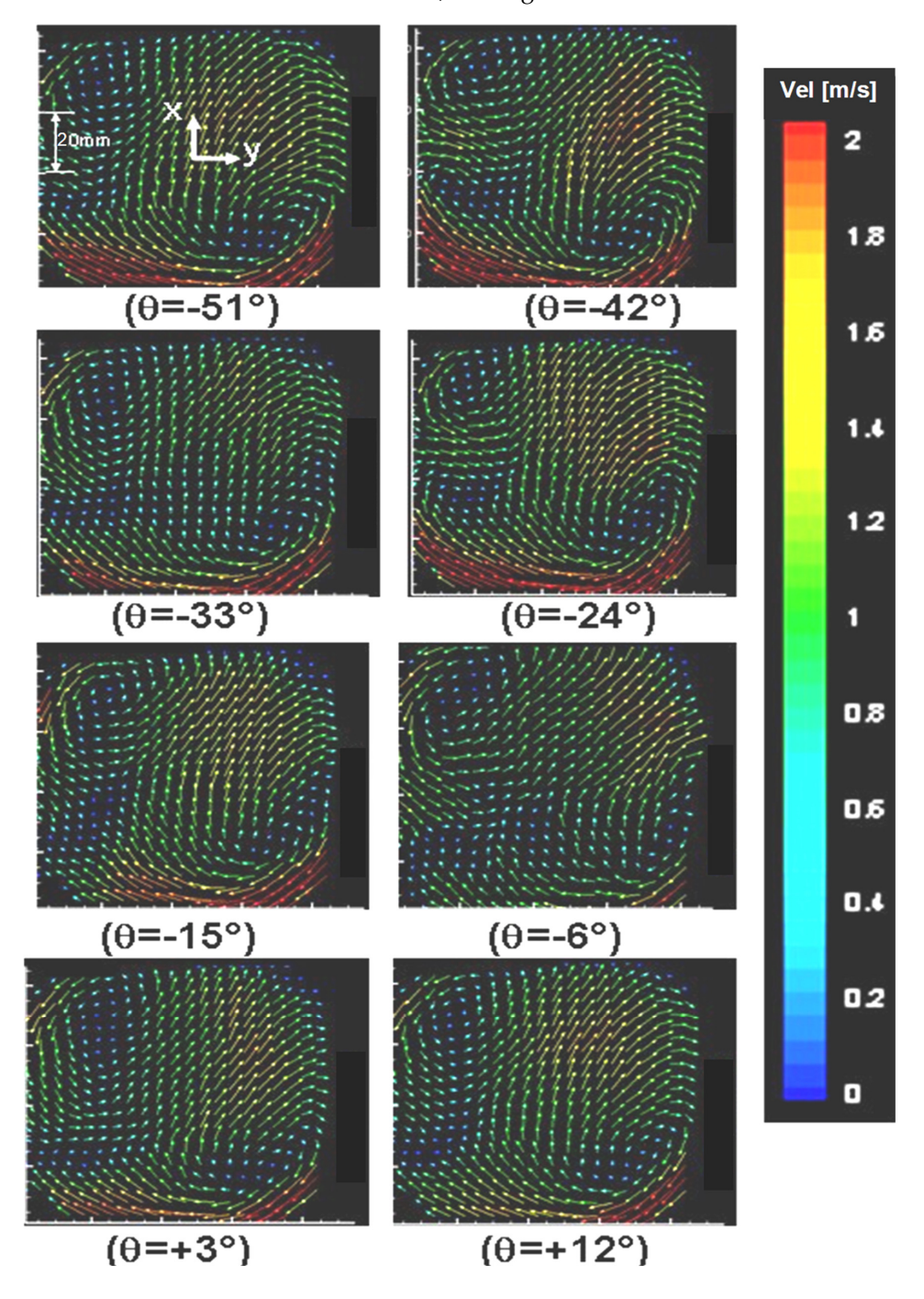


Figure 10. Mean vector velocity variation of axial (Vx) and horizontal (Vy) velocities within the X-Y plane at different shaft angles, θ , and at Z = 75 mm.

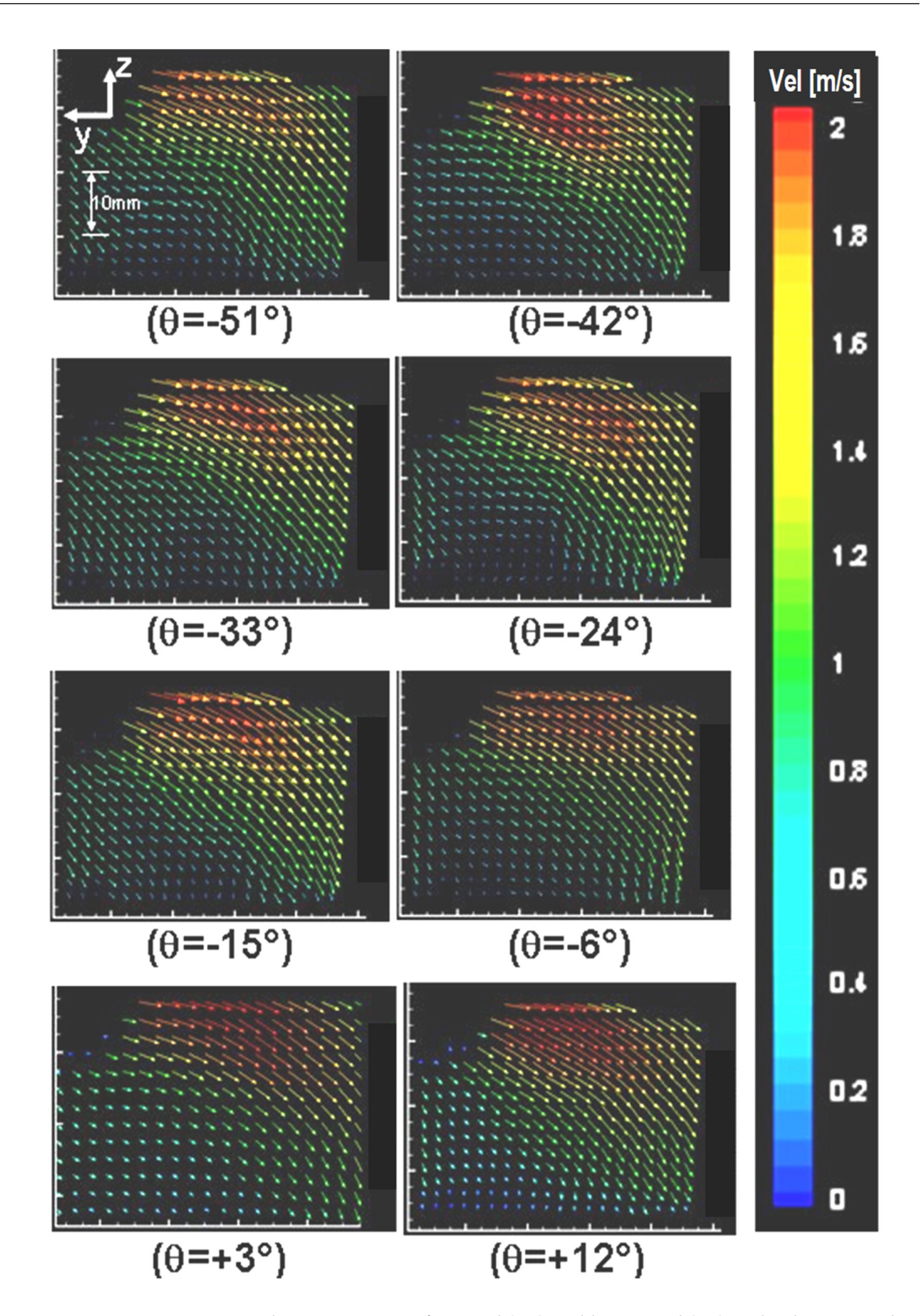


Figure 11. Mean vector velocity variation of vertical (Vz) and horizontal (Vy) and velocities within the Y-Z plane at different shaft angles, θ , and at X = 0 mm.

Figure 11 shows the distribution of mean vector velocity $\left(\sqrt{V_y^2 + V_z^2}\right)$ of axial and vertical velocity components within the Y-Z plane, covering 40 mm above the suction port entrance at eight different shaft angles, θ , and at X = 0 mm. Note that the arrows in the image do not represent the true origin of the coordinate system, as the origin is hidden within the compressor; the one shown in the top left picture is only to indicate flow directions. Again, the expectation was to see the flow as more vertical and uniform, moving downwards towards the rotors, but the results show a more complex flow structure caused

by the lack of flow development in the cylinder, as explained above. The results show similar flow structures at all θ , with no influence from shaft movement. At the top of the images, there is a relatively strong stream with almost horizontal vectors pointing to the right, which suggest that the flow is dominated by the Vy velocity component. Then, as the flow moves downwards, the velocities become more and more vertical. At the very bottom of the images, near the suction port, the flow is almost entirely vertical. Due to the fact that the PIV system requires two directions of operation (here, horizontal and vertical), it was not possible to obtain results closer to the rotors than those shown at the bottom of each image in Figure 11; such measurements are possible using LDV in back-scattering mode. This shows how a single-point measurement system such as LDV is far more adaptable in environments with limited optical access. On the other hand, where access is available, PIV offers an unbeatable solution with high spatial resolution. Thus, it is recommended to modify the suction port, as mentioned before, to provide more optical access for PIV measurements. Overall, the limited PIV results within the suction port highlighted detailed mean flow structures with reasonable temporal and spatial resolutions. It should also be noted that the data sampling for PIV measurements is smaller than those for LDV, which makes it difficult to fully capture the turbulent flow structure with high accuracy. Therefore, the combined LDV/PIV measurement allows better flow analysis for such highly complex, transient, turbulent, and unsteady flow within screw compressors. Nevertheless, a sample of axial, horizontal, and vertical velocity fluctuations are presented and discussed in Figures 12 and 13.

Figures 12 and 13 provide the results of turbulence RMS velocities at the same spatial locations as those in Figures 10 and 11, respectively. Eight images are chosen, corresponding to different shaft angles, which are enough to guarantee a good analysis because LDV results showed that the flow is almost independent of the shaft angles. Results show the contour distributions of the axial and horizontal velocity fluctuation components in Figure 12, and of the horizontal and vertical velocity fluctuation components in Figure 13. From Figure 12 the RMS values are, on average, around 1 m/s, and are reasonably uniform across the X-Y plane at all shaft angles and almost independent of the measured component. It is interesting to note that the RMS values for the axial and horizontal velocity fluctuation components are found to be within a similar range to LDV results presented in Figures 8 and 9, despite the higher statistical uncertainties with PIV measurements, as mentioned earlier.

The results of Figure 13 show slightly higher RMS values on the order of 1.5 m/s, and in some local regions, turbulence reaches up to 2 m/s in magnitude, especially for the vertical component (Vz). Part of the observed turbulence is possibly due to the fact that, as the flow exits the feeding pipe and enters the vertical cylinder, some turbulence is generated and carried downward. The results also show that the turbulence levels at the suction port are much lower than those obtained at the discharge port [15–17], by an order of magnitude, mainly due to the complex and 3D mean flow structure with large mean velocity variations and, thus, very steep velocity gradients in the discharge port. In addition, the current results within the inlet cylinder and suction port may suggest that the height of the vertical cylinder is too short to allow uniform flow development at the inlet, but there are also geometrical limitations to consider, such as the maximum operating distance that LDV laser beams can penetrate into the port. However, as the fluid approaches the compressor inlet port, as displayed in Figures 10 and 11, the perturbations are considerably reduced, and it is unlikely that the inlet pipeline is affecting the overall compressor performance.

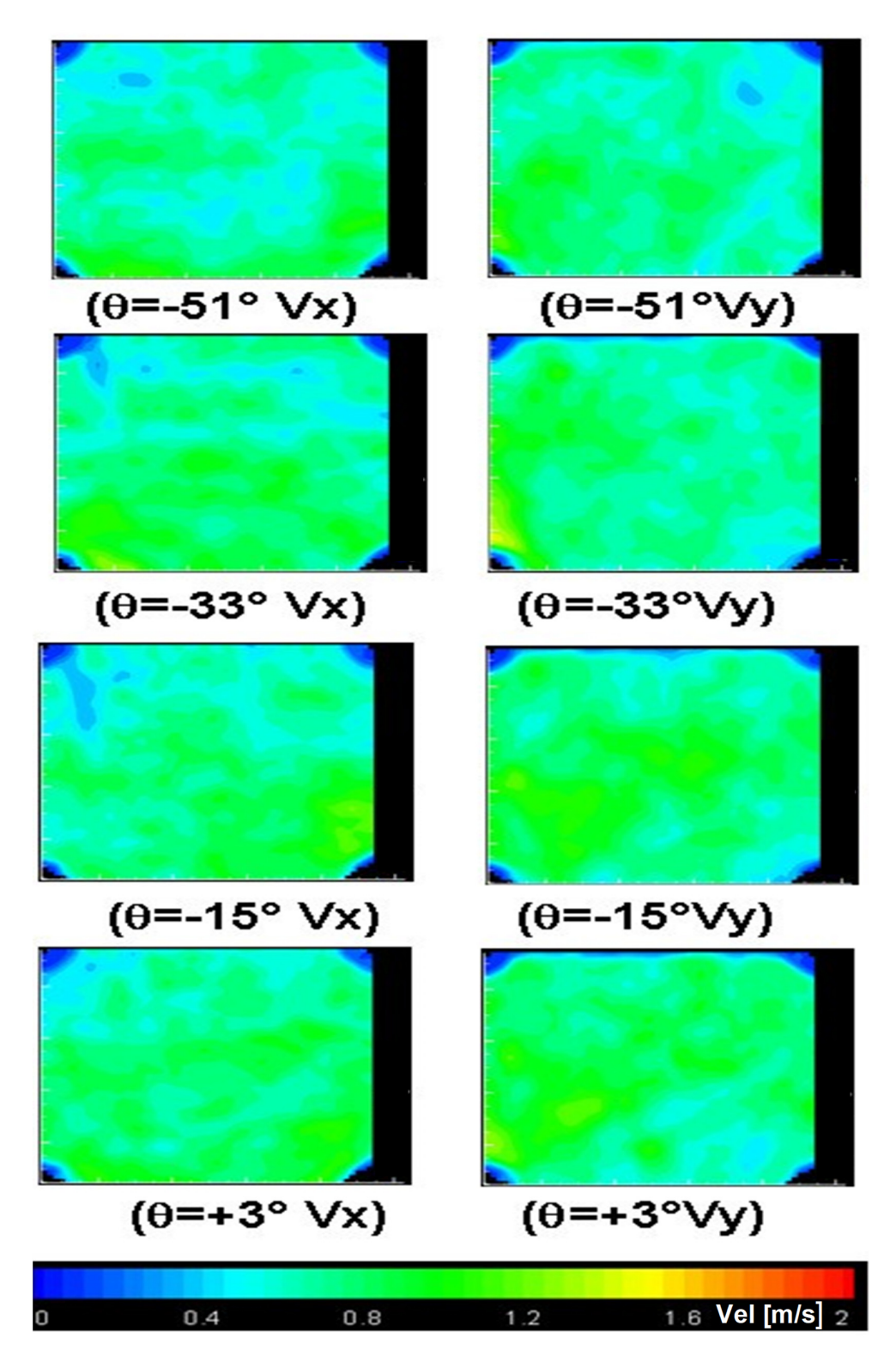


Figure 12. PIV measurement and contours of axial (Vx) and horizontal (Vy) RMS velocity distributions within the X-Y plane at different shaft angles, θ , and at Z = 75 mm.

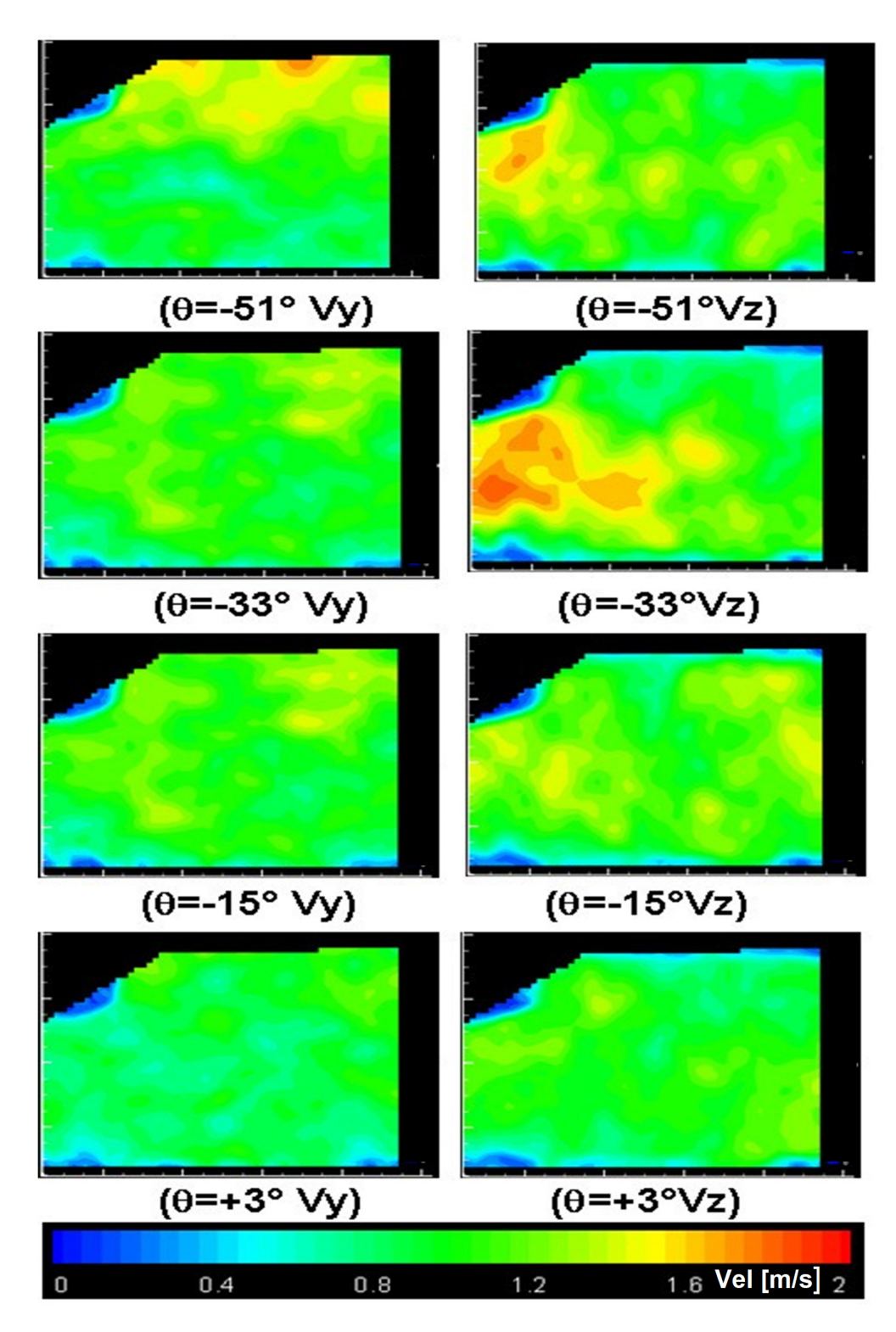


Figure 13. PIV measurement and contours of horizontal (Vy) and vertical (Vz) RMS velocity distributions within the Y-Z plane at different shaft angles, θ , and at X = 0 mm.

4. Conclusions

Mean flow velocities and the corresponding turbulence fluctuation velocities have been measured within the suction port of a standard twin-screw compressor using LDV and PIV optical methods. Time-resolved velocity measurements were carried out over a time window of 1° ($\Delta\theta$) at a rotor speed of 1000 rpm, a pressure ratio of 1, and a gas temperature of 55 °C. The application of LDV and PIV systems to measure mean and

turbulent flow velocities was found to be very successful and presents a novel approach for future research investigations, considering the imposed geometrical and optical access limitations. A summary of the main findings obtained in this research programme is presented below.

4.1. LDV Findings

- The mean vertical velocity (Vz) component at Z = +75 mm (upstream) along the X and Y axes showed uniform downflow velocity profiles with values up to 1.4 m/s with no influence from the rotors' rotational motion on the measured values. Similarly, the rotors' motion had no impact on mean axial and horizontal velocity components at Z = +5 mm (entrance to the port), with low velocity values and uniform profiles.
- At Z = -10 mm, the influence of the rotors' motion on the mean axial (Vx) and horizontal (Vy) velocity components is evident due to its close proximity to the rotors, especially on the axial velocity, forming wave-like profiles with positive values up to 1.8 m/s, while the horizontal velocities were positive (towards male rotor) or negative (towards female rotor) and formed a rotational flow motion with its centre close to the Z axis (centre of the suction cylinder). The results also showed that both Vx and Vy velocity components were influenced by the transverse locations along X and Y axes.
- In addition, the tracking of the measured Vx and Vy velocities at z = -10 mm showed the presence of a complex flow in the suction port that included an axial component moving down towards the rotors' working chambers at the front of the compressor, and that the male rotor interacted better with the air flow within the suction port, causing more air to flow towards the male rotor.
- The results of all measured turbulence velocity fluctuations showed uniform distributions and were independent of the rotor motion, even at Z = -10 mm, the closest measured position to the rotors. The results also showed similar RMS values for all measured components, suggesting that the turbulence can be assumed to be isotropic.

4.2. PIV Findings

- The distribution of mean vector velocity of axial and horizontal velocity components in the X-Y horizontal plane at Z = +75 mm showed similar flow structures at all measured shaft angles, confirming that there is no influence from shaft movement on the flow features. The results also revealed, at all θ positions, the presence of a complex flow with a dominant main stream flow and two counter-rotating vortices at the top left and bottom right of the images; this was due to the undeveloped inlet cylinder flow.
- The distribution of mean vector velocity of axial and vertical velocity components within the Y-Z vertical plane at X = 0 mm showed similar flow structures at all measured shaft angles with no influence from rotor motions, and that the flow consisted of relatively strong horizontal stream flows on the top of all images. As the flow moved down towards the suction port, the velocities became more and more vertical, so at the very bottom of all images, near the suction port entrance, flow was almost entirely vertical.
- The contour results of turbulence velocity fluctuations in both the X-Y horizontal and Y-Z vertical planes displayed fairly uniform distributions, and the axial and horizontal RMS values were found to be within a similar range to LDV results, despite the higher statistical uncertainties associated with PIV measurements.

Author Contributions: J.M.N.: conceptualization, writing, and preparation—original draft, writing—review and editing, supervision, funding acquisition; D.G.: methodology, software, formal analysis, writing—original draft; N.S.: conceptualization, writing—review and editing, supervision,

funding acquisition; Y.Y.: software, formal analysis, writing—review and editing. All authors have read and agreed to the published version of the manuscript.

Funding: This research was founded by The Engineering and Physical Sciences Research Council, EPSRC, under grant number (EP/C541457/1).

Institutional Review Board Statement: Not applicable.

Informed Consent Statement: Not applicable.

Data Availability Statement: The original contributions presented in this study are included in the article. Further inquiries can be directed to the corresponding author(s).

Acknowledgments: We acknowledge the financial support from EPSRC **(Grant No. EP/C541457/1)**. The authors would also like to thank Tom Fleming, Michael Smith, Jim Ford, and Grant Clow for their valuable technical support during the course of this work.

Conflicts of Interest: The authors whose names are listed in the manuscript certify that they have no conflicts of interest. It is also confirmed that the manuscript has been read by all named authors.

References

- Nouri, J.M.; Guerrato, D.; Stosic, N.; Yan, Y. Application of LDV and PIV for flow measurements in the suction port of a screw compressor. In Proceedings of the IOP Conference Series: Materials Science and Engineering, 12th International Conference on Compressors and their Systems (Compressors 2021), London, UK, 6–8 September 2021; Volume 1180, p. 012034.
- Arjeneh, M.; Kovacevic, A.; Rane, S.; Manolis, M.; Stosic, N. Numerical and Experimental Investigation of Pressure Losses at Suction of a Twin Screw Compressor. In Proceedings of the IOP Conference Series: Materials Science and Engineering, 9th International Conference on Compressors and their Systems, London, UK, 7–9 September 2015; Volume 90, p. 012006.
- 3. Stosic, N. Review article: Screw compressors in refrigeration and air conditioning. HVAC R Res. 2004, 10, 233–263. [CrossRef]
- 4. Stosic, N. On gearing of helical screw compressor rotors. *Proc. Inst. Mech. Eng. Part C J. Mech. Eng. Sci.* **1998**, 212, 587–594. [CrossRef]
- 5. Guerrato, D. Cycle-Resolved flow Characterisitcs Within a Screw Compressor. Ph.D. Thesis, University of London, London, UK, 2012.
- 6. Wang, Y.; Xiong, L.; Feng, D.; Liu, X.; Zhao, S. Research progress on the Manufacturing of screw-shaped parts in screw compressors. *Appl. Sci.* **2024**, *14*, 1945. [CrossRef]
- 7. Li, Y.; Zhao, X.; Liu, S.; Wang, C.; Shen, S.; Guo, Y. Review and prospects of numerical simulation research on internal flow and performance optimization of twin-screw compressors. *Energies* **2025**, *18*, 2608. [CrossRef]
- 8. Brinas, I.; Popescu, F.D.; Andras, A.; Radu, S.M.; Cojanu, L. A computerized analysis of flow parameters for a twin-screw compressor using SolidWorks flow simulation. *Computation* **2025**, *13*, 189. [CrossRef]
- 9. Yakupov, R.; Mustafin, T. Comparing of different methods of screw compressor rotors' thermal deformation calculation. In Proceedings of the 14th International Conference on Compressors and their Systems, London, UK, 8–10 September 2025.
- Barrubeeah, M.S.; Bhaduri, S.; Low, D.; Valencic, A.; Groll, E.A.; Ziviani, D. Systematic optimization of screw compressor rotor profiles using and ML-assisted global optimizer. In Proceedings of the 14th International Conference on Compressors and their Systems, London, UK, 8–10 September 2025.
- 11. Tuffaha, S.; Klotsche, K.; Thomas, C.; Hesse, U. Structural dynamics and resonance avoidance in Hi-speed spindle screw compressors. In Proceedings of the 14th International Conference on Compressors and their Systems, London, UK, 8–10 September 2025.
- 12. Guerrato, D.; Nouri, J.M.; Stosic, N.; Arcoumanis, C. Axial flow and pressure characteristics within a double screw compressor. In Proceedings of the 3rd International Conference on Optical and Laser Diagnostics, ICOLD, London, UK, 23–25 May 2007.
- Pascu, M.; Heiyanthuduwage, M.; Mounoury, S.; Cook, G.; Kovacevic, A. A study on the influence of the suction arrangement on the performance of twin screw compressors. In Proceedings of the ASME 2013 International Mechanical Engineering Congress and Exposition, IMECE2013, San Diego, CA, USA, 15–21 November 2013.
- 14. Mujic, E.; Stosic, N.; Smith, I.K. The CFD Analysis of a screw compressor suction flow. In Proceedings of the 15th International Compressor Engineering Conference, West Lafayette, IN, USA, 25–28 July 2000.
- 15. Nouri, J.M.; Guerrato, D.; Stosic, N.; Arcoumanis, C. Axial Flow Characteristics within a Screw Compressor. *ASHRAE Res. J.* **2008**, 14, 259–274. [CrossRef]
- 16. Nouri, J.M.; Guerrato, D.; Stosic, N. Turbulent flow measurements near the discharge port of a screw compressor. *Int. J. Flow Turbul. Combust.* **2020**, *104*, 927–946. [CrossRef]

17. Nouri, J.M.; Guerrato, D.; Stosic, N.; Yan, Y. Turbulent flow development within the discharge cavity of a screw compressor. *Int. J. Engine Res.* **2023**, *24*, 3642–3654. [CrossRef]

- 18. Marchi, A.; Yan, Y.; Nouri, J.M.; Arcoumanis, C. PIV Investigation on Flows Induced by Fuel Sprays from an Outwards Opening Pintle Injector for GDI engines. In Proceedings of the International Conference ILASS, Ghania, Greece, 1–4 September 2013.
- 19. Patel, H.; Lakhera, V.J. A critical review of experimental studies related to twin screw compressors. *Proc. Inst. Mech. Eng. Part E J. Process. Mech. Eng.* **2019**, 234, 157–170. [CrossRef]
- 20. Mujic, E.; Kovacevic, A.; Stosic, N.; Smith, I.K. The Influence of discharge ports on rotor contact in screw compressor. In Proceedings of the 18th International Compressor Engineering Conference, West Lafayette, IN, USA, 17–20 July 2006.
- 21. Bikramaditya, N.; Rane, S.; Kovacevic, A.; Patel, B. CFD analysis of leakage flow in radial tip gap of roots blower. In *Book: 13th International Conference on Compressors and Their Systems*; Springer: Cham, Switzerland, 2024; pp. 35–46. [CrossRef]
- 22. Bikramaditya, N.; Rane, S.; Kovacevic, A.; Omidyeganeh, M. Development of CFD model for radial leakage flow in a roots blower and validation using particle image velocimetry. *J. Results Eng.* **2025**, *26*, 105578. [CrossRef]
- 23. Tsao, C.C.; Lin, W.K.; Lai, K.Y.; Yavuzkurt, S.; Liu, Y.H. Numerical investigation of compression and expansion process of twin-screw machine using R-134a. *Energies* **2023**, *16*, 3599. [CrossRef]
- 24. Marchi, A. Internal Flow and Spray Characteristics of an Outwards Opening Pintle-Type Gasoline-Injector. Ph.D. Thesis, University of London, London, UK, 2009.
- 25. Peng, X.; Xing, Z.; Zhang, X.; Shu, P. Experimental study of oil injection and its effect on performance of twin screw compressor. In Proceedings of the 15th International Compressor Engineering Conference, West Lafayette, IN, USA, 25–28 July 2000.
- 26. Toyama, T.; Matsuura, H.; Yoshida, Y. Visual Techniques to quantify behaviour of oil droplets in a scroll compressor. In Proceedings of the 18th International Compressor Engineering Conference, West Lafayette, IN, USA, 25–28 July 2006.
- 27. Jassal, G.R.; Schmidt, B.E. Error-based dynamic velocity range of PIV processing algorithms. Exp. Fluids 2025, 66, 68. [CrossRef]

Disclaimer/Publisher's Note: The statements, opinions and data contained in all publications are solely those of the individual author(s) and contributor(s) and not of MDPI and/or the editor(s). MDPI and/or the editor(s) disclaim responsibility for any injury to people or property resulting from any ideas, methods, instructions or products referred to in the content.